components of $\Delta z/|\Delta z|$ remain finite as $|\Delta z| \to 0$ and τ can be evaluated. The value of τ thus obtained depends on the relative magnitudes of the components z_i. If we consider an n-dimensional "configuration" space, in which each coordinate axis represents z_i, then any nonequilibrium state of the system (under constant T and p) can be represented by a point in this configuration space. Equation 6 describes the motion of such a representative point in it. Given sufficient time, trajectories of all representative points will eventually converge to a single point corresponding to the equilibrium state. The same material system having different thermal histories will initially be placed at different regions of the configuration space, and the trajectories, as they approach the equilibrium point, will be different from each other. Consequently, the values of τ given by eq 7 will also be different from each other.

The above discussion shows that the main point depicted in Figure 1, i.e., the limiting τ values of volume relaxation to depend on previous thermal history, can be explained without assuming that the state reached after prolonged annealing is something different from a true equilibrium state. It is also conceivable that volume is a very insensitive indicator of attainment of equilibrium. If that is the case, then even when volume has apparently reached its limit, the structure may still be far from true equilibrium and continues to undergo slow relaxation. As evidence supporting this, we can cite the observation[20] that the shape of the endothermic peak of annealed polystyrene, obtained by differential scanning calorimetry, continues to change long after the volume relaxation has achieved apparent completion.

Acknowledgment. A helpful criticism, on an earlier manuscript of this work, by Dr. J. J. Aklonis is gratefully acknowledged. This work was supported in part by the National Science Foundation under Grants DMR77-20876 and DMR80-04236.

References and Notes

(1) Guinier, A. "X-ray Diffraction"; W. H. Freeman: San Francisco, 1963; p 46. Guinier, A.; Fournet, G. "Small-Angle Scattering of X-rays"; Wiley: New York, 1955; p 71.
(2) Wendorff, J. H.; Fischer, E. W. *Kolloid Z. Z. Polym.* **1973**, *251*, 876.
(3) Rathje, J.; Ruland, W. *Colloid Polym. Sci.* **1976**, *254*, 358.
(4) See Matyi et al. (Matyi, R. J.; Uhlmann, D. R.; Koutsky, J. A. *J. Polym. Sci., Polym. Phys. Ed.* **1980**, *18*, 1053) for the reference to the series of papers on this subject by Uhlmann and co-workers.
(5) Wendorff, J. H. *J. Polym. Sci., Polym. Lett. Ed.* **1979**, *17*, 765.
(6) Curro, J. J.; Roe, R. J., unpublished work.
(7) Kovacs, A. J. *J. Polym. Sci.* **1958**, *30*, 131.
(8) A. J. Kovacs, *Fortschr. Hochpolym. Forsch.* **1963**, *3*, 394.
(9) Adam, G. *Kolloid Z. Z. Polym.* **1962**, *180*, 11.
(10) Bueche, F. *J. Chem. Phys.* **1962**, *36*, 2940.
(11) Hozumi, S. *Polym. J.* **1971**, *2*, 756.
(12) Narayanaswamy, O. S. *J. Am. Ceram. Soc.* **1971**, *54*, 491.
(13) Kovacs, A. J.; Hutchinson, J. M.; Aklonis, J. J. In "Proceedings of the Symposium on the Structure of Non-crystalline Materials"; Cambridge University Press: New York, 1976; p 153.
(14) Debolt, M. A.; Easteal, A. J.; Macedo, P. B.; Moynihan, C. T. *J. Am. Ceram. Soc.* **1976**, *59*, 16.
(15) Kovacs, A. J.; Aklonis, J. J.; Hutchinson, J. M.; Ramos, A. R. *J. Polym. Sci., Polym. Phys. Ed.* **1979**, *17*, 1097.
(16) Robertson, R. E. *J. Polym. Sci., Polym. Symp.* **1978**, *63*, 173. *J. Polym. Sci., Polym. Phys. Ed.* **1979**, *17*, 597.
(17) de Groot, S. R.; Mazur, P. "Non-Equilibrium Thermodynamics"; North-Holland Publishing Co.: Amsterdam, 1962, p 221.
(18) Davies, R. O.; Jones, G. O. *Adv. Phys.* **1953**, *2*, 370.
(19) Roe, R. J. *J. Appl. Phys.* **1977**, *48*, 4085.
(20) Curro, J. J.; Roe, R. J. *Bull. Am. Phys. Soc.* **1980**, *25*, 283. Curro, J. J. M.S. Thesis, University of Cincinnati, 1979.

Static Scattering Function for a Polymer Chain in a Good Solvent

TAKAO OHTA,[1A,C] YOSHITSUGU OONO,[1B,C] and KARL F. FREED*[1B]

Department of Physics, University of Pittsburgh, Pittsburgh, Pennsylvania 15260, Department of Physics, Kyushu University, Fukuoka 812, Japan, and The James Franck Institute and the Department of Chemistry, The University of Chicago, Chicago, Illinois 60637.
Received November 24, 1980

The most directly measurable quantity that is related to the spatial structure of a single polymer chain in a good solvent is the static scattering function $S(\mathbf{k})$, which is given by

$$S(\mathbf{k}) = \sum_{i=1}^{N}\sum_{j=1}^{N}\langle \exp[i\mathbf{k}\cdot(\mathbf{c}_i - \mathbf{c}_j)]\rangle \tag{1}$$

where $\mathbf{c}_i$ denotes the position of the ith monomer and $\langle\ \rangle$ the equilibrium ensemble average. Experimental determinations focus on the ratio $I(\mathbf{k}) = S(\mathbf{k})/S(\mathbf{0})$. Let $x = k^2\langle S^2\rangle$, where $\langle S^2\rangle$ is the mean-square radius of gyration and $k = |\mathbf{k}|$. Then $I(x)$ is a universal function of x. For a Gaussian chain, the ratio $I_0(x)$ is given by

$$I_0(x) = 2\left(\frac{1}{x} + \frac{e^{-x}}{x^2} - \frac{1}{x^2}\right) \tag{2}$$

Witten and Schäfer[2] recently used renormalization theory to calculate the leading two nontrivial terms in the series expansion of $I(x)$ in powers of x to order $\epsilon = 4 - d$, where d is the spatial dimension. They note that $I_0(x) > I(x)$ for smaller x. In the $x \to \infty$ limit these scattering functions behave as $I(x) \sim x^{-1/2\nu}$ ($\nu \sim {}^3/_5$) and $I_0(x) \sim x^{-1}$, but this appears to occur beyond the currently accessible experimental range, i.e., for $x > 100$. In this limit $I(x) > I_0(x)$, and as is noted by Witten and Schäfer,[2] there must be an x_c such that $I(x_c) = I_0(x_c)$.

We provide a closed-form expression for $I(x)$ to order ϵ for fully developed excluded volume. The result is obtained for all values of x, the limiting $x \to 0$ and $x \to \infty$ regions, and the intermediate regime that is inaccessible to scaling theories. Our calculational method is based on the Gell-Mann–Low type renormalization group theory, which is formulated in chain configuration space.[3] The theoretical details will be published elsewhere;[4] here we concentrate on the final results. The closed form of $I(x)$ is given by

$$I(x) = e^{-\epsilon/8}f(\beta) \tag{3}$$

where

$$\beta = dx/3(1 - 13\epsilon/96)$$

and

$$f(\beta) = I_0(\beta)\exp[-\epsilon g(\beta)/4I_0(\beta)]$$

$$g(\beta) = 2\int_0^1 dt\left[\frac{e^{-\beta}}{\beta^2}A[\beta - \beta t(1-t)] + \left(\frac{1}{\beta} - \frac{1}{\beta^2}\right)A(-\beta t(1-t)) - \frac{1 - \exp[-\beta t(1-t)]}{\beta^2 t(1-t)}\right] + \int_0^1 dt\left[\frac{1}{\beta(1-t)} + \frac{\exp[-\beta t(1-t)] - 1}{\beta^2 t(1-t)^2}\right] - \frac{1}{\beta^2}e^{-\beta}A(\beta) + \frac{1}{\beta}e^{-\beta}A(\beta) + \frac{1}{\beta}e^{-\beta}$$

$$A(x) = \int_0^x dt\ (e^t - 1)/t$$

0024-9297/81/2214-1588$01.25/0

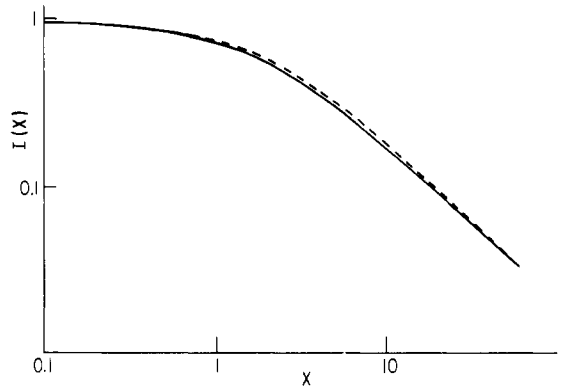

Figure 1. Comparison of $I(x)$ and $I_0(x)$ in 3-space. $x = k^2\langle S^2\rangle$. The dashed line denotes I_0 and the solid line I. Therefore, the value of x differs for I and I_0 at a given k. $I(x)$ and $I_0(x)$ cross each other around $x_c \simeq 10^2$.

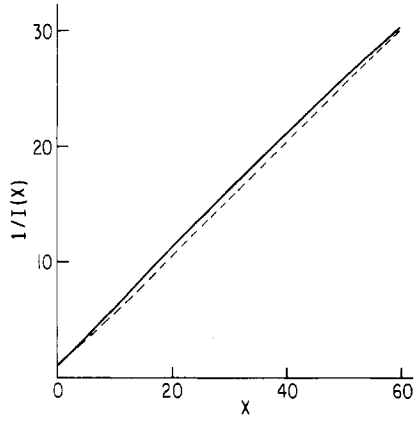

Figure 2. $I(x)^{-1}$ vs. x in 3-space. The dashed line denotes I_0^{-1} and the solid line I^{-1}.

$I(x)$ at $\epsilon = 1$ (i.e., in 3-space) and $I_0(x)$ are displayed as functions of x in Figure 1. They are very similar. Note that x differs in magnitude between I_0 and I for a fixed value of **k**. $I(x)$ and $I_0(x)$ become equal at around $x_c = 10^2$. However, since the coefficient of ϵ in the x–β relation is rather large, the present estimate of x_c is not too reliable. because $I(x)$ is slightly flatter than $I_0(x)$, the density profile of the self-avoiding polymer is more compact than the Gaussian polymer. This observation is in accordance with the differences of the end-to-end vector distribution functions for both cases.[3,5]

Figure 2 is a plot of $I(x)^{-1}$ vs. x. Note that $I(x)^{-1}$ is definitely *larger* than $I_0(x)^{-1}$ for a wide range of x. This is contrary to existing theoretical and experimental results,[6,7] except for the theoretical work of Witten and Schäfer.[2,8] Possible reasons for this discrepancy are discussed below. Figure 3 displays the dissymmetry factor $q_{\pi/4}$ defined by

$$q_{\pi/4} = I\left[\left(4\pi \sin\frac{\pi}{8}\right)^2 Y^2\right] \Big/ I\left[\left(4\pi \sin\frac{3\pi}{8}\right)^2 Y^2\right] \quad (4)$$

with $Y = \langle S^2\rangle^{1/2}/\lambda$, where λ is the wavelength of the light. $q_{\pi/4}$ lies well below the $q^0{}_{\pi/4}$ for the Gaussian chain. However, the asymptotic relation $I(x) \sim x^{-1/2\nu}$ gives $\lim_{y\to\infty} q_{\pi/4} = [\sin(3\pi/8)/\sin(\pi/8)]^{1/\nu}$, i.e., 4.676... to order ϵ (or 4.3447... using $\nu = {}^3/_5$) for the polymer chain with full excluded volume. This is to be compared with the value 5.828... for the Gaussian chain. Therefore, again there must be some $Y = Y_c$ where $q_{\pi/4} = q^0{}_{\pi/4}$. This Y_c seems very large. $q_{\pi/4}$ for rods lies well above $q^0{}_{\pi/4}$, while $q_{\pi/4}$ for spheres is below $q^0{}_{\pi/4}$. This suggests that at least globally, i.e., in the range $Y < Y_c$, the self-avoiding polymer

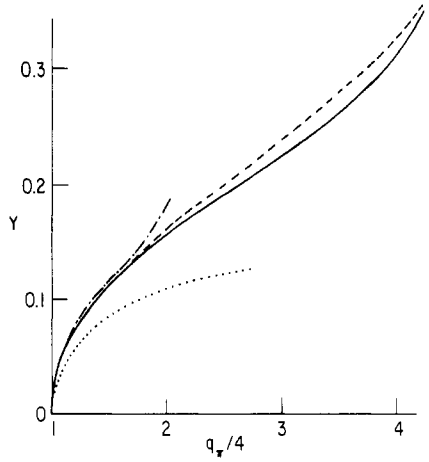

Figure 3. Dissymmetry factor $q_{\pi/4}$ in 3-space: (—) self-avoiding chain; (– – –) Gaussian chain; (···) sphere; (–·–) rod. $Y = \langle S^2\rangle^{1/2}/\lambda$. For the sphere and rod the radius of gyration is used as $\langle S^2\rangle$; i.e., $Y \approx 0.316D$ for a sphere of diameter D and $Y \approx 0.289L$ for a rod of length L. At least for smaller Y, the full curve lies between the broken and dotted curves. This suggests that the self-avoiding chain is more spherical than the simple random walk chain. The corrections of $O(\epsilon^2)$ will shift the full curve toward the Gaussian chain curve, but the qualitative feature will remain intact.

chain is more spherical than the Gaussian chain because of the self-repulsion. Monte Carlo calculations, on the other hand, exhibit the moments of inertia of self-avoiding chains as being less spherical than the Gaussian chain.[8] These facts are not in conflict, however, since the light scattering and the moments of inertia provide different measures of "sphericity".

The difference between the calculated and experimental relative magnitudes of $I_0(x)$ and $I(x)$ for $x < x_c$ is a more serious question which must be studied by further theoretical and experimental analyses for the following reasons. Comparing the $Y \to \infty$ limit of $q_{\pi/4}$ between the order ϵ calculation and the expected limit for $\nu = {}^3/_5$ implies that the higher order contributions in ϵ must shift the Y vs. $q_{\pi/4}(y)$ curve upward toward that of the Gaussian chain. This, in turn, leads to $I(x)$ being shifted upward toward the Gaussian $I_0(x)$. There is, of course, the possibility that the shift is great enough to reverse the orders of these curves to be in accord with experiments, but this is believed to be unlikely. The order ϵ calculated for the end-to-end vector distribution function already exhibits all the salient features of the function and is in semiquantiative agreement with the estimate due to Domb, Gillis, and Wilmers.[9] Hence, the major change anticipated in order ϵ^2 is an improvement of the exponent ν. Likewise, the order ϵ^2 corrections to $I(x)$ are not expected to larger than the order ϵ terms as necessary to reverse the relative magnitudes of $I(x)$ and $I_0(x)$. The net conclusion is that $I(x)$ and $I_0(x)$ are sufficiently close to each other such that their differences for $x < x_c$ are probably unmeasurable. The differences in $q^0{}_{\pi/4}$ are more likely to be experimentally discernible. Difficulties in comparing experiment with theory arise from a number of sources. Polydispersity tends to shift the $I(x)^{-1}$ vs. x curve downward. A crucial step in analyzing the experimental data involves the determ ation of $\langle \mathbf{S}^2\rangle$. The latter is often overestimated,[10] further shifting the $I(x)^{-1}$ vs. x curve downward. In addition, the theory here applies to the asymptotic limit of very good solutions and high molecular weights, and the dependence on excluded volume for intermediate excluded volume should be studied.

Acknowledgment. We are grateful to Professor Tomo-o Oyama of Kyushu University for useful comments

and to Dr. Michael Morse for help with the numerical calculations. T.O. is also grateful to Professor D. Jasnow for his hospitality at the University of Pittsburgh. This work is supported, in part, by NSF Grants DMR 78-26630 (Polymers Program) and DMR 76-19443.

References and Notes

(1) (a) University of Pittsburgh. (b) The University of Chicago. (c) Kyushu University. On leave of absence from Kyushu University, Fukuoka, Japan.
(2) Witten, T. A., Jr.; Schäfer, L., preprint.
(3) Oono, Y.; Ohta, T.; Freed, K. F. *J. Chem. Phys.* **1981**, *74*, 6458.
(4) Ohta, T.; Oono, Y.; Freed, K. F., submitted to *Phys. Rev. A.*
(5) Oono, Y.; Ohta, T.; Freed, K. F., submitted to *Macromolecules.*
(6) Ptitsyn, O. B. *Zh. Fiz. Khim.* **1957**, *31*, 1091.
(7) See e.g.: McIntyre, D.; Mazur, J.; Wims, A. M. *J. Chem. Phys.* **1968**, *49*, 2887, 2896. Mijnlieff, P. F.; Coumon, D. J.; Meisner, J. *Ibid.* **1970**, *53*, 1775.
(8) Rubin, R. J.; Mazur, J. *J. Chem. Phys.* **1975**, *63*, 5362.
(9) Domb, C.; Gillis, J.; Willmers, G. *Proc. Phys. Soc., London* **1965**, *85*, 625.
(10) Professor T. Oyama, private communication.

On Frenkel's Governor Model for Stretched Polymers

J. H. WEINER* and D. PERCHAK

Division of Engineering and Department of Physics, Brown University, Providence, Rhode Island 02912.
Received April 10, 1981

The usual discussion of the force required to maintain a long-chain molecule at a fixed length is based on the concept of entropy, an approach in which the fundamental basis for the resulting force is not easily accessible to one's physical intuition. In an attempt to provide an explanation of what he termed the kinetic origin of the force, Frenkel[1] introduced the atomistic analogue of a centrifugal governor. The model consists of a chain of three atoms with fixed bond length a and the two end atoms fixed at a distance $2l$ apart, Figure 1. If it is assumed that the central atom is in thermal motion with a velocity corresponding to its mean kinetic energy of $^1/_2kT$, then it is easily derived by elementary mechanics[1,2] that the required force f is

$$f = \frac{l}{2(a^2 - l^2)}kT \tag{1}$$

a result which shows the dependence upon temperature and upon end-to-end length which is typical of a long-chain molecule under tension. The same force–length–temperature relation can be derived more formally on the basis of classical equilibrium statistical mechanics. The Hamiltonian of the model in terms of the angle coordinate θ (Figure 1) and corresponding momentum p_θ is

$$H_r(\theta,p_\theta) = \frac{1}{2}\frac{p_\theta^2}{mr^2} \tag{2}$$

where

$$r = (a^2 - l^2)^{1/2} \tag{3}$$

and the corresponding partition function is, with $\beta = (kT)^{-1}$

$$\begin{aligned} Z_r(l,T) &= \int_0^{2\pi} d\theta \int_{-\infty}^{\infty} e^{-\beta p_\theta^2/2mr^2}\, dp_\theta \\ &= 2\pi(2\pi mkT)^{1/2}(a^2 - l^2)^{1/2} \end{aligned} \tag{4}$$

Therefore the required force is

$$f_r = -\frac{\partial}{\partial(2l)}kT \log Z_r(l,T) = \frac{l}{2(a^2 - l^2)}kT \tag{5}$$

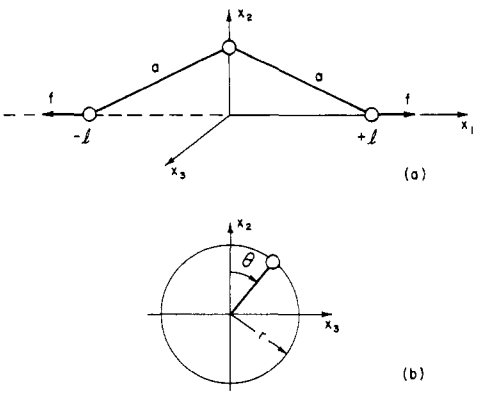

Figure 1. Two-bond model of stretched polymer. (a) End atoms are maintained at fixed positions $x_1 = \pm l$ by axial force f while the central atom is in thermal motion. In the rigid model, bond lengths are fixed at a and the central atom moves on a circle of radius $r = (a^2 - l^2)^{1/2}$ in the x_2–x_3 plane as shown in (b). The position of the central atom is then described in terms of the angle coordinate θ.

as before.

Frenkel's model is, in present terminology, a rigid polymer model in the sense that the fixed bond length a is imposed first in the Hamiltonian of the model and the partition function is computed subsequently; the subscript r on H, Z, and f has been added in order to emphasize that these quantities apply to the rigid case. The corresponding flexible model is obtained if in the model Hamiltonian H_f the bond lengths are held approximately constant by means of stiff linear springs with spring constant κ, the partition function Z_f is computed on the basis of H_f, and κ is allowed to become arbitrarily large in the resulting expression.

There have been a number of recent studies devoted to the comparison of the statistical behavior of rigid and flexible models,[3-7] and for some cases, striking differences have been demonstrated by computer simulation.[8-10] These works have been directed primarily at free molecules in solution. It is the purpose of this note to consider the flexible version of Frenkel's model and to compare its force–length–temperature relation with that for the corresponding rigid model.

The Hamiltonian for the flexible model may be described in terms of a rectangular Cartesian coordinate system, with $\mathbf{x}$ the position and $\mathbf{p}$ the momentum of the moving atom, as

$$H_f(\mathbf{x},\mathbf{p}) = \frac{1}{2m}|\mathbf{p}|^2 + V(\mathbf{x}) \tag{6}$$

where

$$V(\mathbf{x}) = \tfrac{1}{2}\kappa[(|\mathbf{x} - \mathbf{l}| - a)^2 + (|\mathbf{x} + \mathbf{l}| - a)^2] \tag{7}$$

Here κ is the linear spring constant and $\pm\mathbf{l}$ are the positions of the fixed atoms. The corresponding partition function is

$$\begin{aligned} Z_f(l,T) &= \int_{\Gamma_p} e^{-\beta|\mathbf{p}|^2/2m}\, d\mathbf{p} \int_{\Gamma_x} e^{-\beta V(\mathbf{x})}\, d\mathbf{x} \\ &= (2\pi mkT)^{3/2} \int_{\Gamma_x} e^{-\beta V(\mathbf{x})}\, d\mathbf{x} \end{aligned} \tag{8}$$

where the integration over momentum space Γ_p has been performed. To evaluate the integral over the configuration space Γ_x, we use the fact that for large κ, $V(\mathbf{x})$ is large except when $\mathbf{x}$ is in the neighborhood of a point on the circle of radius $r = (a^2 - l^2)^{1/2}$ at an arbitrary angle θ as in Figure 1. We introduce local rectangular Cartesian coordinates (ξ,η) with origin on this circle in the plane of $-\mathbf{l},\mathbf{x},\mathbf{l}$,

0024-9297/81/2214-1590$01.25/0